

ELECTRON–HOLE EXCHANGE INTERACTION IN A SPHERICAL QUANTUM DOT WITH REGARD MATERIAL DEFORMATION AND POLARIZATION CHARGES

R. Ya. Leshko¹, I. V. Bilynskyi^{1,2}, O. V. Leshko¹

¹*Physics Department, Drohobych Ivan Franko State Pedagogical University,
3, Stryiska St., Drohobych, UA-82100, Ukraine,*

²*Physics Department, Kryvyi Rih State Pedagogical University,
54, Gagarin Ave., Kryvyi Rih, UA-50086, Ukraine
e-mail: leshkoroman@gmail.com*

(Received 25 November 2021; in final form 08 February 2022; accepted 22 February 2022; published online 30 March 2022)

The focus of the study is on the strained spherical quantum dot (QD) InAs/GaAs heterosystem. A singleband model of the conductive band for electrons and a multiband model of the valence band for holes have been applied. Both models take into account the deformation of the QD and matrix and polarization charges on the boundaries. The proposed models have been used for the calculation of the electron–hole exchange interaction.

Key words: exchange interaction, deformation, multiband model, polarization charges, strained heterosystem.

DOI: <https://doi.org/10.30970/jps.26.1702>

I. INTRODUCTION

For the last 20 years, the redshift of the emission spectra with respect to absorption spectra (Stokes shift) in the QD has been observed experimentally by many researchers [1–6]. Understanding the nature of this effect is important in modern optoelectronic technologies. That is why there are a lot of theoretical explanations of the redshift in the QD. They have been presented in many works, for example [7–11]. The generalized results of those and other works suggest several reasons for the Stokes shift explanation. One of them is the exchange electron–hole interaction. The comprehensive theory of the exchange electron–hole interaction in the QD and its results are presented in [7]. According to [7], electron states are twofold degenerate, while the hole ground state corresponding to the value of the total momentum 3/2 is fourfold degenerate. So without taking into account any interactions, the ground state of the electron–hole pair is eightfold degenerate. The electron and the hole are connected by the Coulomb interaction. According to general rules of adding momentum moments, the electron–hole pair can have values of the total momentum 1, 2. In this case, the state with 1 is optically active (“light”), and the state with 2 is inactive (“dark”) in the dipole approximation. The difference between the energies of dark–light states is defined by the exchange interaction. Also in works [8–11], the dielectric mismatch and polarization charges at QD–matrix interfaces are taken into account. In [10], it was shown that if the dielectric permittivity of the matrix is larger than in the QD one, the energy of the electron–hole exchange interaction decreases compared with the case when the dielectric permittivity of the matrix is smaller than in the QD. But in [10] only the singleband model for holes was used, which has some inaccuracies compared with the multiband model. Therefore, in this article we will use the multiband model, which improves

the obtained results. As a rule, InAs QDs are obtained by heteroepitaxial growth in the Frank–van der Merwe regime or the Volmer–Weber regime or the Stranski–Krastanow regime. Due to the lattice mismatch of InAs and GaAs during the heteroepitaxial growth on a crystal substrate, the strained InAs QDs are formed [12]. So the deformation of the QD has an effect on the optical properties and electron–hole exchange interaction too. There are many reports where the effect of the lattice deformation of the InAs QD is considered, for example [13–16]. In our work [16] it has been shown that polarization and deformation caused an opposite effect on the energy of the electron and the hole spectrum of InAs/GaAs QDs. Therefore, we assume that deformation and polarization have to influence the electron–hole exchange interaction too. Thus the aim of this paper is to determine the electron–hole exchange interaction in the QD InAs/GaAs heterosystem with regard to deformation and polarization effects and compare it in singleband and multiband models.

II. HETEROSYSTEM MODEL

Let us consider the InAs/GaAs heterosystem with a coherent strained spherical InAs QD of the radius a . The QD is assumed to be an elastic dilatational sphere. It is inserted into a spherical void in the GaAs matrix (the volume of the void is smaller than that of the nanoinclusion by ΔV) [13–15]. Electrons and holes are confined by the rectangular potential well

$$U_{\text{conf}}(r_j) = \begin{cases} 0, & r_j \leq a, \\ U_{0;j} & r_j > a, \end{cases}, j = e, h. \quad (1)$$

In this and other equations, the index j takes the values e, h (electron and hole) For holes, the energy axis in the valence band is directed “downward”. The change



of the renormalized potential energy by the hydrostatic deformation is presented by

$$\Delta U_j^{(i)} = D_j^{(i)} \varepsilon^{(i)}, \quad (2)$$

where $\varepsilon^{(i)} = \text{Sp}(\tilde{\varepsilon}^{(i)})$; $\tilde{\varepsilon}^{(i)}$ is the deformation tensor; $D_j^{(i)}$ are constants of the hydrostatic deformation potential of the conduction band and the valence band, $i = 1$ (InAs), 2 (GaAs). Therefore, the potential energies of the hole and the electron caused by deformation are defined as

$$U_d(r_j) = \begin{cases} 0, & r_j \leq a, \\ U_{0,d;j} & r_j > a, \end{cases} \quad (3)$$

where $U_{0,d;j} = -|D_j^{(1)} \varepsilon^{(1)}| - |D_j^{(2)} \varepsilon^{(2)}|$. $\varepsilon^{(i)}$ are defined as in [14, 15, 18, 19] and do not depend on \vec{r} . The mediums are described by their own dielectric permittivity (χ_1, χ_2). According to [17], we obtain the potential energy of the interaction of the charge particle with polarization charges as follows:

$$U_p(r_j) = \frac{\gamma_0}{4\chi(r_j)} \int_0^\infty dr_0 \frac{\tanh(w(r_0)) + r_0/L \cdot \text{sech}(w(r_0))}{r_0^2 - r_j^2}, \quad (4)$$

$$\chi(r_j) = \frac{\chi_1 + \chi_2}{2} [1 - \gamma_0 \tanh(w(r_j))], \quad (5)$$

$$\gamma_0 = \frac{\chi_1 - \chi_2}{\chi_1 + \chi_2}, \quad w(r_j) = \frac{r_j - a}{L}, \quad (6)$$

$L \approx a_0^{(1)}/4$, where $a_0^{(1)}$ is the lattice constant of InAs. In all formulas we use the Hartree system of units ($\hbar = 1, e = 1, m_0 = 1$). Therefore, the total potential energy consists of the confinement potential U_{conf} (1), deformation potential U_d (2), and polarization potential U_p (4).

$$U = U_{\text{conf}} + U_d + U_p. \quad (7)$$

In the next chapter, we solve the Schrödinger equation for the electron and the hole in a potential field (7).

III. ELECTRONS AND HOLES SPECTRA

In the singleband effective mass approximation, the electron Hamiltonian has the form

$$\begin{aligned} \hat{\mathbf{H}}_e &= -\frac{1}{2} \nabla \frac{1}{m_e} \nabla + U(r_e) \\ &= -\frac{1}{2} \nabla \frac{1}{m_e} \nabla + U_{\text{conf}}(r_e) + U_d(r_e) + U_p(r_e) \\ &= \hat{\mathbf{H}}_e^0 + U_d(r_e) + U_p(r_e), \end{aligned} \quad (8)$$

where

$$m_e = \begin{cases} m_e^{(1)}, & r_e \leq a, \\ m_e^{(2)}, & r_e > a. \end{cases}$$

If $U_d = 0$ and $U_p = 0$, polarization and deformation effects are neglected. The Schrödinger equation with and without taking into account the QD deformation can be solved exactly. For the ground state, it has a solution expressed by the wave function:

$$\psi_{e;m_s}(\vec{r}_e) = \frac{1}{\sqrt{4\pi}} S_{e;m_s} r_e^{-1} \begin{cases} A_e^{(1)} \sin(kr_e), & r_e \leq a, \\ A_e^{(2)} \exp(-\eta r_e) & r_e > a, \end{cases} \quad (9)$$

where $S_{e;m_s}$ is a spin function, $m_s = \pm 1/2$, $k = \sqrt{2m_e^{(1)}E}$. When the QD deformation is neglected, $\eta = \sqrt{2m_e^{(2)}(U_{0,e} - E)}$, and $\eta = \sqrt{2m_e^{(2)}(U_{0,e} + U_{0,d;e} - E)}$, if the QD deformation is taken into account. From the Ben Daniel–Duke boundary conditions and normalization condition, coefficients $A_e^{(1)}$, $A_e^{(2)}$ and the electron energy can be defined with and without taking into account the QD deformation. To calculate (4), the Ritz variational method has been used. The trial function has been chosen in the form:

$$\psi_{e;m_s}^{(V)}(\vec{r}_e) = \frac{1}{\sqrt{4\pi}} S_{e;m_s} R_e^{(V)}(r_e) = \frac{1}{\sqrt{4\pi}} S_{e;m_s} r_e^{-1} \begin{cases} A_e^{(1,V)} \sin(\alpha r_e), & r_e \leq a, \\ A_e^{(2,V)} \exp(-\beta r_e) & r_e > a. \end{cases} \quad (10)$$

From the boundary conditions, we got:

$$A_e^{(1,V)} = A_e^{(2,V)} \exp(-a\beta) \sec(\alpha a), \quad (11)$$

$$\beta = \frac{m_e^{(1)} - m_e^{(2)} + m_e^{(2)} \alpha a \cot(\alpha a)}{a m_e^{(1)}}, \beta > 0. \quad (12)$$

So the trial function has two parameters $A_e^{(2,V)}$ and α .

Variational parameter α and the electron ground state energy have been defined by the minimization of the functional

$$G_e(\alpha) = \frac{\langle \psi_{e;m_s}^{(V)}(\vec{r}_e) | \hat{\mathbf{H}}_e | \psi_{e;m_s}^{(V)}(\vec{r}_e) \rangle}{\langle \psi_{e;m_s}^{(V)}(\vec{r}_e) | \psi_{e;m_s}^{(V)}(\vec{r}_e) \rangle}. \quad (13)$$

$A_e^{(2,V)}$ has been defined from the normalized condition. Hamiltonian (8) does not depend on spin variables; thus, the electron energy does not depend on spin too. Therefore, we defined the ground electron state with and without taking into account both deformation and polarization effects. In the same manner, the hole ground state can be defined in the singleband model. To improve quantitative results for the hole states, the multiband model of the valence band should be used. We use the multiband model with a strong spin-orbit interaction to calculate the hole states [20–23]. The hole (light and heavy holes) effective masses in every environment are

$m_{\text{lh}}^{(1)}, m_{\text{hh}}^{(1)}$ and $m_{\text{lh}}^{(2)}, m_{\text{hh}}^{(2)}$ respectively. The energy axis in the valence band is directed “downward” (the maximum of the valence band transforms into the minimum). If we neglect the corrugation of the isoenergetic surfaces in the k-space, the Hamiltonian of the hole is given by

$$\hat{\mathbf{H}}_h = \frac{1}{2} \left(\gamma_1 + \frac{5}{2} \gamma \right) \hat{\mathbf{p}}^2 - \gamma (\vec{\mathbf{p}} \cdot \vec{\mathbf{J}})^2 + U(r_h), \quad (14)$$

where $\vec{\mathbf{p}}$ is the momentum operator, $\vec{\mathbf{J}} = \vec{i}\hat{\mathbf{J}}_x + \vec{j}\hat{\mathbf{J}}_y + \vec{k}\hat{\mathbf{J}}_z$ is the spin operator ($j = 3/2$), γ_1 and γ are the Luttinger parameters which are connected with the heavy and light hole effective masses

$$m_{\text{hh}} = \frac{1}{\gamma_1 - 2\gamma}, \quad m_{\text{lh}} = \frac{1}{\gamma_1 + 2\gamma}. \quad (15)$$

The solution of the Schrödinger equation with Hamiltonian (14) for the hole ground state (if we assume, that $U_p(r_h) = 0$) has the form [7, 8, 16, 24]:

$$\begin{aligned} \psi_{h;M}(r_h, \theta_h, \varphi_h) &= 2 \sum_{l=0,2} (-1)^{M-3/2} R_l(r_h) \sum_{m_l, m_j} \begin{pmatrix} l & 3/2 & 3/2 \\ m_l & m_j & -M \end{pmatrix} Y_{l, m_l}(\theta_h, \varphi_h) S_{h; m_j} \\ &= R_0(r_h) |l=0, j=3/2, f=3/2, M\rangle + R_2(r_h) |l=2, j=3/2, f=3/2, M\rangle. \end{aligned} \quad (16)$$

$\vec{\mathbf{F}} = \vec{\mathbf{L}} + \vec{\mathbf{J}}$ is the total angular momentum, $f(f+1)$, $l(l+1)$, M, m, m_j in this system of units are the eigenvalues of operators $\hat{\mathbf{F}}^2$, $\hat{\mathbf{L}}^2$, $\hat{\mathbf{F}}_z$, $\hat{\mathbf{L}}_z$, $\hat{\mathbf{J}}_z$, respectively; $S_{h; m_j}$ are the spin functions; Y_{l, m_l} are the spherical harmonic functions, which are the eigenfunctions of $\hat{\mathbf{L}}^2$; $\begin{pmatrix} l & 3/2 & 3/2 \\ m_l & m_j & -M \end{pmatrix}$ are the 3-j symbols. If $r_h \leq a$ (the QD region), radial functions can be expressed by the sum of the Bessel functions of the first kind [24]

$$R_0^{(1)}(r_h) = A_{1;h}^{(1)} \frac{-J_{1/2}(k_{\text{hh}}^{(1)} r_h)}{\sqrt{r_h}} + A_{2;h}^{(1)} \frac{J_{1/2}(k_{\text{lh}}^{(1)} r_h)}{\sqrt{r_h}}, \quad (17)$$

$$R_2^{(1)}(r_h) = A_{1;h}^{(1)} \frac{J_{5/2}(k_{\text{hh}}^{(1)} r_h)}{\sqrt{r_h}} + A_{2;h}^{(1)} \frac{J_{5/2}(k_{\text{lh}}^{(1)} r_h)}{\sqrt{r_h}}, \quad (18)$$

where $k_{\text{hh}}^{(1)} = \sqrt{2m_{\text{hh}}^{(1)} E}$, $k_{\text{lh}}^{(1)} = \sqrt{2m_{\text{lh}}^{(1)} E}$. If $r_h > a$ (the matrix region), radial functions can be expressed in terms of the modified Bessel functions of the second kind

$$R_0^{(2)}(r_h) = A_{1;h}^{(2)} \frac{K_{1/2}(k_{\text{hh}}^{(2)} r_h)}{\sqrt{r_h}} + A_{2;h}^{(2)} \frac{-K_{1/2}(k_{\text{lh}}^{(2)} r_h)}{\sqrt{r_h}}, \quad (19)$$

$$R_2^{(2)}(r_h) = A_{1;h}^{(2)} \frac{K_{5/2}(k_{\text{hh}}^{(2)} r_h)}{\sqrt{r_h}} + A_{2;h}^{(2)} \frac{K_{5/2}(k_{\text{lh}}^{(2)} r_h)}{\sqrt{r_h}}, \quad (20)$$

where $k_{\text{hh}}^{(2)} = \sqrt{2m_{\text{hh}}^{(2)}(U_{0;h} - E)}$, $k_{\text{lh}}^{(2)} = \sqrt{2m_{\text{lh}}^{(2)}(U_{0;h} - E)}$, if the deformation is neglected, and $k_{\text{hh}}^{(2)} = \sqrt{2m_{\text{hh}}^{(2)}(U_{0;h} + U_{0;d;h} - E)}$, $k_{\text{lh}}^{(2)} = \sqrt{2m_{\text{lh}}^{(2)}(U_{0;h} + U_{0;d;h} - E)}$, if the deformation is taken into account. The radial solution, boundary conditions [16, 24, 25] and normalization conditions were applied to determine the energy levels with and without taking into account the deformation effect. To calculate (4) for the hole states within the multiband approximation, the Ritz variational method has been used. Trial radial functions have been chosen in the form:

$$R_0^{(1,V)}(r_h) = A_{1;h}^{(1,V)} \frac{-J_{1/2}(\alpha \sqrt{m_{\text{hh}}^{(1)}} r_h)}{\sqrt{r_h}} + A_{2;h}^{(1,V)} \frac{J_{1/2}(\alpha \sqrt{m_{\text{lh}}^{(1)}} r_h)}{\sqrt{r_h}}, \quad (21)$$

$$R_2^{(1,V)}(r_h) = A_{1;h}^{(1,V)} \frac{J_{5/2}(\alpha \sqrt{m_{hh}^{(1)}} r_h)}{\sqrt{r_h}} + A_{2;h}^{(1,V)} \frac{J_{5/2}(\alpha \sqrt{m_{lh}^{(1)}} r_h)}{\sqrt{r_h}}, \quad (22)$$

if $r_h \leq a$. If $r_h > a$:

$$R_0^{(2,V)}(r_h) = A_{2;h}^{(1,V)} \frac{K_{1/2}(\beta \sqrt{m_{hh}^{(2)}} r_h)}{\sqrt{r_h}} + A_{2;h}^{(2,V)} \frac{-K_{1/2}(\beta \sqrt{m_{lh}^{(2)}} r_h)}{\sqrt{r_h}}, \quad (23)$$

$$R_2^{(2,V)}(r_h) = A_{2;h}^{(1,V)} \frac{K_{5/2}(\beta \sqrt{m_{hh}^{(2)}} r_h)}{\sqrt{r_h}} + A_{2;h}^{(2,V)} \frac{K_{5/2}(\beta \sqrt{m_{lh}^{(2)}} r_h)}{\sqrt{r_h}}. \quad (24)$$

Boundary conditions for the multiband model [16, 24, 25] give four equations. From those equations we defined:

$$A_{2;h}^{(1,V)} = g_1(\alpha, A_{1;h}^{(1,V)}),$$

$$A_{1;h}^{(2,V)} = g_2(\alpha, A_{1;h}^{(1,V)}),$$

$$A_{2;h}^{(2,V)} = g_3(\alpha, A_{1;h}^{(1,V)}),$$

$$\beta = g_4(\alpha, A_{1;h}^{(1,V)}).$$

Those parameters have been substituted into (21)–(24). Thus the total trial wave function depends on $\alpha, A_{1;h}^{(1,V)}$:

$$\begin{aligned} \psi_{h;M}^{(V)}(\vec{r}_h) = & R_0^{(V)}(r_h; \alpha, A_{1;h}^{(1,V)}) |l=0, j=3/2, f=3/2, M\rangle + \\ & + R_2^{(V)}(r_h; \alpha, A_{1;h}^{(1,V)}) |l=2, j=3/2, f=3/2, M\rangle. \end{aligned} \quad (25)$$

The hole energy and parameter α have been defined by the minimization of the variational functional:

$$G_h(\alpha) = \frac{\langle \psi_{h;M}^{(V)}(\vec{r}_h) | \hat{\mathbf{H}}_h | \psi_{h;M}^{(V)}(\vec{r}_h) \rangle}{\langle \psi_{h;M}^{(V)}(\vec{r}_h) | \psi_{h;M}^{(V)}(\vec{r}_h) \rangle} \quad (26)$$

Due to the spherical symmetry, the hole energy does not depend on M . $A_{1;h}^{(1)}$ has been defined from the normalized condition. For calculation we use the parameters as in [15]. Therefore we defined the ground hole states within the multiband model with and without taking into account both deformation and polarization effects. A similar calculation was done in our previous work [16]. But there we used the perturbation theory to account for polarization. The obtained ground state energies (in this work and in [16]) are very close. The differences do not exceed 2%.

IV. EXCITON MODEL

In the proposed models, the exciton Hamiltonian has the form:

$$\hat{\mathbf{H}}_{\text{exciton}} = \hat{\mathbf{H}}_e + \hat{\mathbf{H}}_h + \hat{\mathbf{H}}_{\text{ex}} + W(\vec{r}_e, \vec{r}_h) + E_g, \quad (27)$$

where E_g is the band gap, $\hat{\mathbf{H}}_{\text{ex}}$ the electron–hole exchange interaction Hamiltonian. $W(\vec{r}_e, \vec{r}_h)$ is the

expression of the electron–hole interaction [27]. It can be divided into two terms (see appendix):

$$W(\vec{r}_e, \vec{r}_h) = W_p(\vec{r}_e, \vec{r}_h) + W_{e-h}(\vec{r}_e, \vec{r}_h), \quad (28)$$

where $W_p(\vec{r}_e, \vec{r}_h)$ (it is proportional to $(\chi_2 - \chi_1)$) is the potential energy which includes the interaction between the hole and the polazition charges (induced by the electron), and the interaction between the electron and the polazition charges (inducted by the hole); $W_{e-h}(\vec{r}_e, \vec{r}_h)$ is the direct Coulumb interaction (see Appendix). Therefore, U_p (4) describes the interaction between the charge particle and its “own” polarization charges, and $W_p(\vec{r}_e, \vec{r}_h)$ describes the interaction between the charge particle and “foreign” polarization charges.

The interaction between the charge particle (electron or hole) and its “own” polarization charges has been taken into account in the previous section in the variational functions of the hole and the electron.

To take into account the $W_p(\vec{r}_e, \vec{r}_h)$ and $W_{e-h}(\vec{r}_e, \vec{r}_h)$, the self-consistent problem should be solved for

- a) the singleband model of both the valence band and the conduction band;
- b) the singleband model of the conduction band and the multiband model of the valence band.

As an example, we present the iterative method for the b) case.

First iteration. First of all, we define:

$$W^{(1)}(\vec{r}_e) = \left\langle \psi_{h;M}^{(V)}(\vec{r}_h) | W(\vec{r}_e, \vec{r}_h) | \psi_{h;M}^{(V)}(\vec{r}_h) \right\rangle. \quad (29)$$

Then we solve the Schrödinger equation:

$$(\hat{\mathbf{H}}_e + W^{(1)}(\vec{r}_e)) \psi_{e;m_s}^{(V,1)}(\vec{r}_e) = E_e^{(1)} \psi_{e;m_s}^{(V,1)}(\vec{r}_e) \quad (30)$$

using the variational method as in (9)–(13). In the next step we define

$$W^{(1)}(\vec{r}_h) = \left\langle \psi_{e;m_s}^{(V,1)}(\vec{r}_e) | W(\vec{r}_e, \vec{r}_h) | \psi_{e;m_s}^{(V,1)}(\vec{r}_e) \right\rangle \quad (31)$$

and solve the Schrödinger equation:

$$(\hat{\mathbf{H}}_h + W^{(1)}(\vec{r}_h)) \psi_{h;M}^{(V,1)}(\vec{r}_h) = E_h^{(1)} \psi_{h;M}^{(V,1)}(\vec{r}_h) \quad (32)$$

using the variational method as in (21)–(26).

Second iteration. In this step, we define

$$W^{(2)}(\vec{r}_e) = \left\langle \psi_{h;M}^{(V,1)}(\vec{r}_h) | W(\vec{r}_e, \vec{r}_h) | \psi_{h;M}^{(V,1)}(\vec{r}_h) \right\rangle \quad (33)$$

and solve the equation as in (30)–(32). The iteration procedure is convergent after 4 iteration steps, when

$$(E_e^{(i)} - E_e^{(i-1)}) / E_e^{(i)} \cdot 100\% < 5\%$$

and

$$(E_h^{(i)} - E_h^{(i-1)}) / E_h^{(i)} \cdot 100\% < 5\%.$$

After that, we got the electron and the hole wave functions which take into account all potential energies: For a) case

$$\psi_{h;m_s^{(h)}}^{(\text{conv})} = \psi_{h;m_s^{(h)}}^{(V,4)}; \quad (34)$$

$$\psi_{e;m_s^{(e)}}^{(\text{conv})} = \psi_{e;m_s^{(e)}}^{(V,4)}. \quad (35)$$

For b) case

$$\psi_{h;M}^{(\text{conv})}(\vec{r}_h) = \psi_{h;M}^{(V,4)}(\vec{r}_h); \quad (36)$$

$$\psi_{e;m_s^{(e)}}^{(\text{conv})} = \psi_{e;m_s^{(e)}}^{(V,4)}. \quad (37)$$

V. ELECTRON-HOLE EXCHANGE INTERACTION

According to the general theory, the electron-hole exchange interaction Hamiltonian has the form [7]:

$$\begin{aligned} \hat{\mathbf{H}}_{\text{ex}} &= -(2/3)E_{\text{ex}}(a_0^{(1)})^3 \delta(\vec{r}_e - \vec{r}_h) (\vec{\sigma} \times \vec{\mathbf{J}}) \\ &= -K \delta(\vec{r}_e - \vec{r}_h) (\vec{\sigma} \times \vec{\mathbf{J}}), \end{aligned} \quad (38)$$

where E_{ex} is the exchange strength constant, which can be defined from equation [4, 7]:

$$\hbar\omega_{\text{st}} = (8/3\pi)(a_0^{(1)}/a_{\text{ex}})^3 E_{\text{ex}},$$

where $a_0^{(1)}$ is the QD lattice parameter, $\hbar\omega_{\text{st}} = 0.0025$ meV [1], a_{ex} is the exciton radius, $\vec{\sigma}$ is the electron Pauli spin-1/2 matrix, $\vec{\mathbf{J}}$ is the hole spin matrix (1/2 in the singleband model of the valence band and 3/2 in the multiband model of the valence band).

Let us consider a singleband model for the valence band and conduction band. Within those models, the electron and the hole have spin 1/2. To define the exchange interaction, we use the electron-hole wave function in the form

$$\psi_{e-h} = \sum_{m_s^{(e)}=-1/2}^{1/2} \sum_{m_s^{(h)}=-1/2}^{1/2} C_{m_s^{(e)}, m_s^{(h)}} \psi_{e;m_s^{(e)}}^{(\text{conv})}(\vec{r}_e) \psi_{h;m_s^{(h)}}^{(\text{conv})}(\vec{r}_h), \quad (39)$$

where $\psi_{e;m_s^{(e)}}^{(\text{conv})}(\vec{r}_e)$ and $\psi_{h;m_s^{(h)}}^{(\text{conv})}(\vec{r}_h)$ are defined by (34). So the matrix of the electron-hole exchange interaction with the use of (39) has the form

$$\begin{pmatrix} Z & 0 & 0 & 0 \\ 0 & -Z & 2Z & 0 \\ 0 & 2Z & -Z & 0 \\ 0 & 0 & 0 & Z \end{pmatrix}, \quad (40)$$

where

$$\begin{aligned} Z &= K \frac{1}{4\pi} \int_0^\infty \left| R_e^{(\text{conv})}(r) \right|^2 \left| R_h^{(\text{conv})}(r) \right|^2 r^2 dr \\ &= (2/3)E_{\text{ex}} \left(a_0^{(1)} \right)^3 \int_0^\infty \left| R_e^{(\text{conv})}(r) \right|^2 \left| R_h^{(\text{conv})}(r) \right|^2 r^2 dr = E_{\text{ex}} I_{\text{sb}} \end{aligned} \quad (41)$$

is an overlap integral. The eigenvalues of (40) define the electron-hole exchange interaction in the singleband model. Therefore, we get four eigenvalues. Three of them are Z . It corresponds to an optically active state with the total

electron–hole spin momentum 1. One eigenvalue is equal to $-3Z$. It corresponds to an optically passive state with the total electron–hole spin momentum 0 (so called dark state). Therefore, in the singleband model of the valence band and conduction band, the 4-fold degenerate electron–hole energy level splits into two levels. The splitting energy is

$$E_{\text{sp}} = 4Z = 4E_{\text{ex}}I_{\text{sb}}. \quad (42)$$

In the multiband model of the valence band, the hole spin is equal to $3/2$. To define the exchange interaction in this case, we use the electron–hole wave function in the form

$$\psi_{\text{e-h}} = \sum_{m_s^{(e)}=-1/2}^{1/2} \sum_{M=-3/2}^{3/2} C_{m_s^{(e)},M} \psi_{e;m_s^{(e)}}^{(\text{conv})}(\vec{r}_e) \psi_{h;M}^{(\text{conv})}(\vec{r}_h), \quad (43)$$

where $\psi_{e;m_s^{(e)}}^{(\text{conv})}(\vec{r}_e)$ and $\psi_{h;M}^{(\text{conv})}(\vec{r}_h)$ are defined by (36). So the matrix of the electron–hole exchange interaction with the use of (43) has the form

$$\begin{pmatrix} -3/2X & 0 & 0 & 0 & 0 & 0 & 0 & 0 \\ 0 & 3/2X & -\sqrt{3}X & 0 & 0 & 0 & 0 & 0 \\ 0 & -\sqrt{3}X & -X/2 & 0 & 0 & 0 & 0 & 0 \\ 0 & 0 & 0 & X/2 & -2X & 0 & 0 & 0 \\ 0 & 0 & 0 & -2X & X/2 & 0 & 0 & 0 \\ 0 & 0 & 0 & 0 & 0 & -X/2 & -\sqrt{3}X & 0 \\ 0 & 0 & 0 & 0 & 0 & -\sqrt{3}X & 3X/2 & 0 \\ 0 & 0 & 0 & 0 & 0 & 0 & 0 & -3/2X \end{pmatrix}, \quad (44)$$

where

$$\begin{aligned} X &= K \frac{1}{40\pi} \int_0^\infty |R_{el}^{(\text{conv})}(r)|^2 \left(10 |R_0^{(\text{conv})}(r)|^2 + 2 |R_2^{(\text{conv})}(r)|^2 \right) r^2 dr \\ &= \frac{2}{3} E_{\text{ex}} (a_0^{(1)})^3 \frac{1}{4\pi} \int_0^\infty |R_{el}^{(\text{conv})}(r)|^2 \left(|R_0^{(\text{conv})}(r)|^2 + 0.2 |R_2^{(\text{conv})}(r)|^2 \right) r^2 dr = E_{\text{ex}} I_{\text{mb}}. \end{aligned} \quad (45)$$

The eigenvalues of (44) define the energy of the electron–hole exchange interaction. Therefore, we get eight eigenvalues. Three of them are $5/2X$. It corresponds to an optically active state with the total electron–hole spin momentum 1. Five eigenvalues are equal to $-3/2X$. It corresponds to an optically passive state with the total electron–hole spin momentum 2 (the so called dark state). Therefore, in the multiband model of the valence band and in the singleband model of the conduction band the 8-fold degenerate electron–hole energy level splits into two levels. The splitting energy which defines the Stokes shift is

$$E_{\text{sp}} = 4X = 4E_{\text{ex}}I_{\text{mb}}. \quad (46)$$

Therefore, in both models the electron–hole exchange interaction causes the energy levels splitting. After calculation, we defined the partial contribution of polarization and deformation to the exchange electron–hole interaction and to the splitting energy. For the calculati-

on, we used the same parameters as in our previous article [16].

In the singleband model of the valence band, we get E_{sp} as the function of the QD radius (Fig. 1). During the calculation, we assumed that the hole masses are equal to the heavy hole mass $m_{\text{hh}}^{(1)}$ and $m_{\text{hh}}^{(2)}$ (the singleband heavy hole model). From Fig. 1 one can see that polarization and deformation cause opposite dependences. The QD-matrix deformation causes a decrease in the splitting energy. The reason for that dependence is the decrease in the overlap integral of the hole and electron functions (41). It can also be explained by different values of constants of the hydrostatic deformation potential. For the electron, its value is $D_e^{(1)} = -5.08$ eV, $D_e^{(2)} = -7.17$ eV, and for the hole, $D_h^{(1)} = 1$ eV, $D_h^{(2)} = 1.16$ eV [15]. Therefore, the deformation potential affects the electron and the hole with a different strength. As a result, the spatial location of the electron and hole wave function is more shifted. That is why the overlap

integral decreases and the splitting energy decreases too (curve 2 in Fig. 1). The polarization charges which are collected on the QD-matrix boundary form the polarization potential (4). It has the same form for the hole and the electron. But if we take into account the polarization potential, we get an opposite effect: the splitting energy increases (curve 3 in Fig. 1). It can be explained by the coordinate dependence of the polarization potential (4) (see Fig. 2 in [26]). Although in [26] another QD heterosystem is considered, the qualitative dependence of the polarization potential is the same, because the dielectric permittivity of the QD is larger than the matrix dielectric permittivity. Potential (4) “pushes” the wave functions of the hole and the electron to the QD boundary from both sides. Therefore, the overlap integral

increases and the splitting energy increases too (curve 3 in Fig. 1) compared with the case when we do not take into account the polarization charges. This result is in good qualitative agreement with the other work [10] on the cubic QD. In that work (Fig. 5 in [10]), the curve 2 shows the electron-hole exchange energy without taking into account the polarization, and the curve 3 shows the electron-hole exchange energy taking into account polarization in the case when the dielectric permittivity of the QD is larger than the matrix dielectric permittivity. Since polarization and deformation have opposite effects, their total effect is partially compensated (curve 4 in Fig. 1). But in this case, the splitting energy is smaller than in the case when both effects of the polarization and deformation are neglected (curve 1 in Fig. 1).

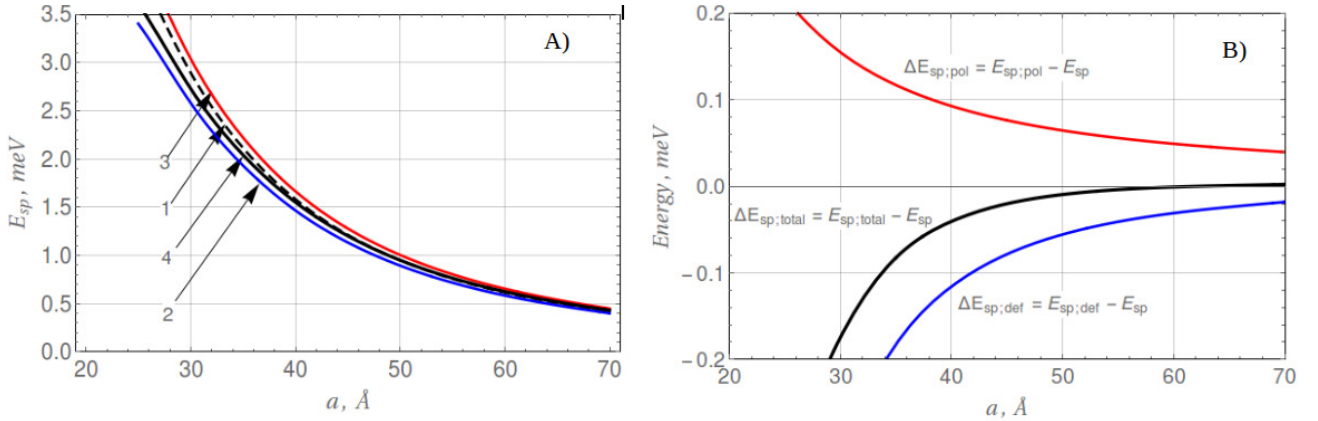


Fig. 1. A) The splitting energy of dark and light exciton states in the singleband model. 1 — without taking into account polarization and deformation effects; 2 — taking into account only QD-matrix deformation; 3 — taking into account only polarization charges; 4 — taking into account both polarization and deformation. B) Partial contributions of: only polarization ($\Delta E_{sp,pol}$), only deformation ($\Delta E_{sp,def}$) and also both polarization and deformation ($\Delta E_{sp,total}$) to the splitting energy

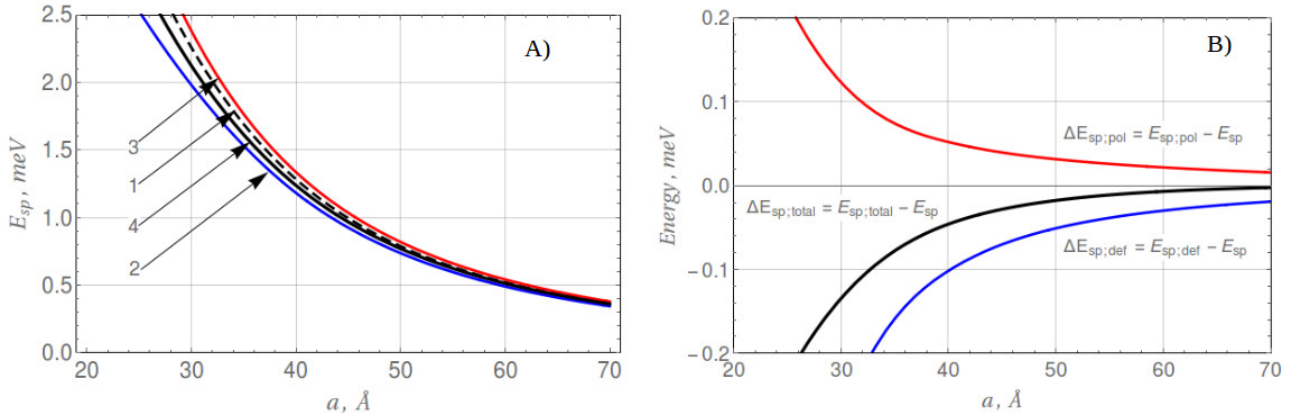


Fig. 2. The splitting energy of dark and light exciton states in the multiband model. 1 — without taking into account polarization and deformation effects; 2 — taking into account only QD-matrix deformation; 3 — taking into account only polarization charges; 4 — taking into account both polarization and deformation. B) Partial contributions of: only polarization ($\Delta E_{sp,pol}$), only deformation ($\Delta E_{sp,def}$) and also both polarization and deformation ($\Delta E_{sp,total}$) to the splitting energy

For the multiband model of the valence band for holes, we got the same qualitative dependence of the splitting energy (Fig. 2) on the QD radius as for the

singleband model. All reasons for the polarization and deformation dependences are the same as in the singleband model. But from Fig. 2 one can see that the spli-

tting energy in the multiband model is smaller than in the singleband one. This dependence is connected with overlap integrals in (45). It has a product of two Bessel functions of the same order $|R_{el}^{(\text{conv})}(r)|^2 |R_0^{(\text{conv})}(r)|^2$ as in the singleband model. Also, the overlap integral has a product of two Bessel functions of the different order $|R_{el}^{(\text{conv})}(r)|^2 |R_2^{(\text{conv})}(r)|^2$. It decreases the overlap integral. That is why in this model the splitting energy is smaller than in the singleband model. In addition, the difference between the two models is the number of light and dark exciton states. In the singleband model, there is one dark state, and in the multiband model there are five of them. The number of light exciton states in both models is three.

VI. CONCLUSION

In this work, we have proposed the singleband model for the conduction band and the multiband model for the valence band. In those models,

we calculated the electron–hole exchange interaction which accounts for the polarization charges on the QD surface and the deformation of the QD and the matrix. For the InAs/GaAs heterosystem, we have shown that deformation leads to a decrease in the splitting energy. If polarization is taken into account, the splitting energy increases in both singleband and multiband models. These two opposite effects partially offset each other. We got that the total effect decreases the splitting energy by 0.12 meV for the QD radius 30 Å and 0.02 meV for the QD radius 50 Å (in the multiband model of the valence band). For the larger QD radii, this difference vanishes. The reason for this dependence is the spatial changes in the electron and hole wave functions. The obtained results can be useful for the theoretical explanation of the Stokes shift value in InAs/GaAs heterosystem. Also, our results for InAs/GaAs are in good agreement with [1] (when polarization and deformation are neglected). The proposed models can be applied to other QDs which can be described by the multiband model with a strong spin-orbit interaction. Also, our model can be expanded for models with a small and intermediate spin-orbit interaction.

APPENDIX

Potential energy of the electron–hole interaction:

$$W(\vec{r}_e, \vec{r}_h) = - \left\{ \begin{array}{l} \frac{\chi_1 - \chi_2}{\chi_1} \sum_{n=0}^{\infty} \frac{n+1}{\chi_1 n + \chi_2(n+1)} \frac{r_e^n r_h^n}{a^{2n+1}} P_n(\cos(\theta)) \\ + \frac{1}{\chi_1} \sum_{n=0}^{\infty} \frac{r_h^n}{r_e^{n+1}} P_n(\cos(\theta)), \quad r_e < a, r_h < a, r_h < r_e, \\ \\ \frac{\chi_1 - \chi_2}{\chi_1} \sum_{n=0}^{\infty} \frac{n+1}{\chi_1 n + \chi_2(n+1)} \frac{r_e^n r_h^n}{a^{2n+1}} P_n(\cos(\theta)) \\ + \frac{1}{\chi_1} \sum_{n=0}^{\infty} \frac{r_e^n}{r_h^{n+1}} P_n(\cos(\theta)), \quad r_e < a, r_h < a, r_e < r_h, \\ \\ \sum_{n=0}^{\infty} \frac{2n+1}{\chi_1 n + \chi_2(n+1)} \frac{r_e^n}{r_h^{n+1}} P_n(\cos(\theta)), \quad r_e < a, r_h > a, \\ \\ \sum_{n=0}^{\infty} \frac{2n+1}{\chi_1 n + \chi_2(n+1)} \frac{r_h^n}{r_e^{n+1}} P_n(\cos(\theta)), \quad r_e > a, r_h < a, \\ \\ \frac{\chi_2 - \chi_1}{\chi_2} \sum_{n=0}^{\infty} \frac{n}{\chi_1 n + \chi_2(n+1)} \frac{a^{2n+1}}{r_e^{n+1} r_h^{n+1}} P_n(\cos(\theta)) \\ + \frac{1}{\chi_2} \sum_{n=0}^{\infty} \frac{r_h^n}{r_e^{n+1}} P_n(\cos(\theta)), \quad r_e > a, r_h > a, r_h < r_e, \\ \\ \frac{\chi_2 - \chi_1}{\chi_2} \sum_{n=0}^{\infty} \frac{n}{\chi_1 n + \chi_2(n+1)} \frac{a^{2n+1}}{r_e^{n+1} r_h^{n+1}} P_n(\cos(\theta)) \\ + \frac{1}{\chi_2} \sum_{n=0}^{\infty} \frac{r_e^n}{r_h^{n+1}} P_n(\cos(\theta)), \quad r_e > a, r_h > a, r_e < r_h, \end{array} \right.$$

where $P_n(x)$ are the Legendre polynomials, \vec{r}_e, \vec{r}_h are the electron and hole coordinates, respectively.

- [1] U. Banin, J. C. Lee, A. A. Guzeliya, A. V. Kadavani, A. P. Alivisatos, *Superlattices Microstruct.* **22**, 559 (1997); <https://doi.org/10.1006/spmi.1997.0504>.
- [2] Jingbo Li, Jian-Bai Xia, *Phys. Rev. B* **61**, 15880 (2000); <https://doi.org/10.1103/PhysRevB.61.15880>.
- [3] T. Warming *et al.*, *Phys. Rev. B* **79**, 125316 (1999); <https://doi.org/10.1103/PhysRevB.79.125316>.
- [4] I. M. Kupchak, D. V. Korbutyak, S. M. Kalytchuk, Yu. V. Kryuchenko, A. Chkrebti, *J. Phys. Stud.* **14**, 2710 (2010); <https://doi.org/10.30970/jps.14.2701>.
- [5] M. S. Gaponenko, N. A. Tolstik, A. A. Lutich, A. A. Onushchenko, K. V. Yumashev, *Physica E* **53**, 63 (2013); <https://doi.org/10.1016/j.physe.2013.04.018>.
- [6] R. Zhou, X. Lub, Q. Yang, P. Wu, *Chin. Chem. Lett.* **30**, 1843 (2019); <https://doi.org/10.1016/j.cclet.2019.07.062>.
- [7] Al. L. Efros *et al.*, *Phys. Rev. B* **54**, 4843 (1996); <https://doi.org/10.1103/PhysRevB.54.4843>.
- [8] A. Yu. Maslov, O. V. Proshina, *Semiconductors* **39**, 1076 (2005); <https://doi.org/10.1134/1.2042602>.
- [9] A. Bagga, P. K. Chattopadhyay, S. Ghosh, *Phys. Rev. B* **74**, 035341 (2006); <https://doi.org/10.1103/PhysRevB.74.035341>.
- [10] V. I. Boichuk, I. V. Bilynskyi, I. O. Shakleina, I. Kogoutiuk, *Physica E* **43**, 161 (2010); <https://doi.org/10.1016/j.physe.2010.06.031>.
- [11] W. Sukkabot, *Superlattices* **105**, 65 (2017); <https://doi.org/10.1016/j.spmi.2017.03.024>.
- [12] N. N. Ledentsov *et al.*, *Semiconductors* **32**, 343 (1998); <https://doi.org/10.1134/1.1187396>.
- [13] M. Grundmann, N. N. Ledentsov, O. Stier, D. Bimberg, *Appl. Phys. Lett.* **68**, 979 (1995); <https://doi.org/10.1063/1.116118>.
- [14] O. O. Dan'kiv, R. M. Peleshchak, *Techn. Phys. Lett.* **31**, 691 (2005); <https://doi.org/10.1134/1.2035368>.
- [15] B. V. Novikov *et al.*, *Semiconductors* **42**, 1076 (2008); <https://doi.org/10.1134/S1063782608090133>.
- [16] R. Ya. Leshko, I. V. Bilynskyi, *Physica E* **115**, 113703 (2020); <https://doi.org/10.1016/j.physe.2019.113703>.
- [17] V. I. Boichuk, R. Yu. Kubai, *Phys. Solid State* **43**, 235 (2001); <https://doi.org/10.1134/1.1349466>.
- [18] L. D. Landau, E. M. Lifshits, *Theory of Elasticity* (Pergamon, New York, 1959).
- [19] Yu. A. Thorik, L. S. Khazan, *Plastic Deformation and Mismatch Dislocations in Heteroepitaxial Systems* (Naukova Dumka, Kyiv, 1983).
- [20] J. M. Luttinger, W. Kohn, *Phys. Rev.* **97**, 869 (1955); <https://doi.org/10.1103/PhysRev.97.869>.
- [21] J. M. Luttinger, *Phys. Rev.* **102**, 1030 (1956); <https://doi.org/10.1103/PhysRev.102.1030>.
- [22] A. Baldereshi, N. O. Lipari, *Phys. Rev. B* **8**, 2697 (1973); <https://doi.org/10.1103/PhysRevB.8.2697>.
- [23] E. Menéndez-Proupin, C. Trallero-Giner, *Phys. Rev. B* **69**, 125336 (2003); <https://doi.org/10.1103/PhysRevB.69.125336>.
- [24] R. Ya. Leshko, I. V. Bilynskyi, *Physica E* **110**, 10 (2019); <https://doi.org/10.1016/j.physe.2019.01.024>.
- [25] E. P. Pokatilov, V. A. Fonoberov, *Phys. Rev. B* **64**, 245328 (2001); <https://doi.org/10.1103/PhysRevB.64.245328>.
- [26] V. I. Boichuk, I. V. Bilynskyi, R. Ya. Leshko, *Condens. Matter Phys.* **11**, 653 (2008); <https://doi.org/10.5488/CMP.11.4.653>.
- [27] V. I. Boichuk, R. Yu. Kubay, H. M. Hodovanets, I. S. Shevchuk, *J. Phys. Stud.* **10**, 220 (2006); <https://doi.org/10.30970/jps.10.220>.

ЕЛЕКТРОН-ДІРКОВА ОБМІННА ВЗАЄМОДІЯ У СФЕРИЧНІЙ КВАНТОВІЙ ТОЧЦІ З УРАХУВАННЯМ ДЕФОРМАЦІЇ МАТЕРІАЛУ ТА ПОЛЯРИЗАЦІЙНИХ ЗАРЯДІВ

Р. Я. Лешко, І. В. Білинський, О. В. Лешко

¹ Кафедра фізики Дрогобицького державного педагогічного університету імені Івана Франка, вул. Стрийська, 3, Дрогобич, 82100, Україна,

² Кафедра фізики Криворізького державного педагогічного університету, проспект Гагаріна, 54, Кривий Ріг, 50086, Україна

Розглянуто напружені сферичні квантові точки гетеросистеми InAs/GaAs. Визначено енергію електрон-діркової обмінної взаємодії. Електронні стани враховано в межах простої параболічної зони провідності (коли можна ввести ізотропну ефективну масу), а діркові - як з урахуванням зони легких та важких дірок одночасно (багатозонна модель), так тільки з урахуванням зони важких дірок (проста зонна модель). В обох моделях урахувано вплив всесторонньої деформації квантової точки внаслідок неузгодження сталих ґратки квантової точки й матриці введенням деформаційного потенціалу. Також визначено вплив поляризаційних зарядів, що виникають на гетеромежі квантова точка-матриця внаслідок різних значень діелектричної проникності квантової точки й матриці. Уведено поляризаційні потенціали, що описують взаємодію заряджених частинок із поляризаційними зарядами, які вони самі створили на гетеромежі квантова точка-матриця. Показано часткові внески поляризації й деформації та їхній спільний вплив на енергію електрон-діркової обмінної взаємодії у квантовій точці. Завдяки обмінній взаємодії відбувається розщеплення екситонних станів на темні та світлі. Визначено енергію розщеплення між цими екситонними станами в простій однозонній та багатозонній моделях як функцію радіуса квантової точки. Показано, що поляризація та деформація чинять протилежні впливи на енергію розщеплення темних і світлих екситонних

станів: поляризація збільшує енергію розщеплення, а деформація її зменшує. Це зумовлює часткову взаємну компенсацію цих ефектів. Однак сумарний їх вплив не нульовий (хоча й незначний). Це пов'язано з тим, що поляризація квантової точки більше змінює енергію розщеплення, ніж її деформація. Зокрема, цей сумарний вплив зменшується зі збільшенням радіуса квантової точки. Наприклад, для радіуса квантової точки 3 нм енергія розщеплення темних і світлих екситонних станів становить 0.12 меВ, а для 5 нм — 0.02 меВ.

Ключові слова: обмінна взаємодія, деформація, багатозонна модель, напружена квантова точка, поляризаційні заряди.